Journal of Inorganic and Organometallic Polymers and Materials (2023) 33:1667–1674
https://doi.org/10.1007/s10904-023-02598-9

RESEARCH

Zinc Zeolite as a Carrier for Tumor Targeted and pH-responsive Drug Delivery

Mariusz Sandomierski[1] · Marcel Jakubowski[1] · Maria Ratajczak[2] · Monika Pokora[3] · Adam Voelkel[1]

Received: 8 August 2022 / Accepted: 26 February 2023 / Published online: 22 March 2023

Abstract
In this work, for the first time, a material was prepared that releases the drug in a controlled manner under the influence of the pH of cancer environment. The material is zinc zeolite, which only releases the drug at an acidic pH. The release of the drug in an acidic environment indicates a very high potential of the synthesized material in the treatment of cancer. This material does not release the drug at pH 7.4 even for more than 100 h which proves that healthy organs will not be affected. The advantage of this material over those previously described in the literature is that it releases the drug very quickly under the influence of the cancerous environment (88% of the drug during approx 2 h), as well as the fact that it does not release the drug in a different environment. Materials with both features have not been previously described, there are only works on materials having one of these features. Moreover, this material releases zinc ions which additionally act on cancer cells by inducing apoptosis of cancer cells by increasing the intracellular production of reactive oxygen species.

Keywords Zinc zeolite · tumor targeted · pH-responsive · controlled release

1 Introduction

Bisphosphonates (BPs) are one of the most important class of drugs used as antiresorptive agents for treatment of metabolic bone related diseases such as osteoporosis, hypercalcemia and Paget's disease [1, 2]. All bisphosphonates used in clinical practice today are geminal bisphosphonates. They are those that in their structure have two bonds between the carbon atom and the phosphorus atom attached to the same carbon atom. This forms a P-C-P bond system, which means that the BPs are analogs of pyrophosphate (P-O-P). Thanks to that they have great chemical and thermal stability [3]. One of the drugs in this class is zoledronate (ZOL), which belongs to the BPs that contain a nitrogen atom in their side chain. Some studies show that it has numerous anti-cancer effects. One of them is the effective inhibition of farnesyl pyrophosphate synthase. It is one of the most important enzymes in mevalonate pathway. Some in vitro studies show that inhibition of the action of this enzyme reduces the proliferation and migration of cancer cells but can also lead to apoptosis. The next anti-cancer activity is that inhibits the signaling of basic fibroblast growth factor and vascular endothelial growth factor, which significantly inhibits blood vessel growth in the tumor. Finally, zoledronate is one of two bisphosphonates that can lead to pyrophotosis, which is one form of programmable cell death [4–6]. The main problem with using zoledronate as an anti-cancer drug is maintaining adequate levels of it in the blood. Like any other bisphosphonate, zoledronate after entering the bloodstream is divided between the bones and kidneys. Zoledronate that go to the kidneys are quickly eliminated from the circulation and expelled from the body unmetabolized in urine [7]. On the other hand, it is impossible to administer higher doses of the drug as it can cause serious side effects [8, 9]. The solution to this problem may be to construct a carrier for zoledronate, which would deliver and release the drug only around the tumor. The release of the ZOL from such a carrier must be relatively quick in order to

✉ Mariusz Sandomierski
mariusz.sandomierski@put.poznan.pl

1 Institute of Chemical Technology and Engineering, Poznan University of Technology, ul. Berdychowo 4, Poznań 60-965, Poland

2 Institute of Building Engineering, Poznan University of Technology, ul. Piotrowo 5, Poznań 60- 965, Poland

3 Center for Advanced Technologies, Adam Mickiewicz University, Poznań, ul. Uniwersytetu Poznańskiego 10, Poznań 61-614, Poland

obtain the appropriate drug concentration at the site of the tumor. It is also known that the pH in the tumor microenvironment is lower than under normal conditions [10, 11]. Zeolites seem to be an ideal candidate for use as a carrier for zoledronate. It is because they are biocompatible materials with lots of biomedical applications, for example: drugs and genes delivery or construction of biosensors [12, 13]. The structure of these materials is made of MO4 tetrahedrons, where M stands for Al or Si. The difference in valence of these two elements causes that the lattice has a negative charge that must be compensated by cations. These cations are exchangeable [10, 14]. There are different type of zeolites but in our work we want to use zeolite X. These type of zeolite is characterized by Si/Al ratio ranging from 1 to 1,5 and pore sizes from 6Å-8Å [15]. In the previous work we proved that zeolites with substituted calcium ions can be used as carriers of risedronate, which belongs to the group of bisphosphonates. Which indicates that bisphosphonates have great affinity to divalent cations [16]. In this paper, we would like to propose a zeolite X-based zoledronate delivery system with Zn^{2+} ions that could release the drug under the influence of the tumor's acidic microenvironment. In addition, it was proved that zinc ions in appropriate concentrations can induce apoptosis of cancer cells by increasing the intracellular production of reactive oxygen species [17]. In our opinion, such a composition will allow for the synergistic anti-cancer effect of zinc ions and zoledronate. This carrier should allow the drug to be delivered to the site of action without releasing the drug to healthy tissue. The scheme of the described studies is shown in Fig. 1.

2 Materials

Sodium zeolite 13X (Na-X, ~2 µm average particle size), zinc chloride, zoledronic acid (-ZOL), sodium chloride (99%), sodium acetate (99%), acetic acid (99%), sodium bicarbonate (99%), sodium sulfate (99%), potassium phosphate dibasic trihydrate (99%), potassium chloride (99%), tris(hydroxymethyl)aminomethane (99%) were obtained from Sigma-Aldrich. Hydrochloric acid (36–38%) was obtained from Avantor. The materials were used without further purification.

2.1 Ion Exchange

Ion exchange was carried out by mixing a 20 ml of 0.5 M solution of the zinc chloride with 1 g of sodium zeolite for 24 h. Then zeolite was centrifuged. This process was repeated three times. After that, zeolite was washed with distilled water to remove excess zinc chloride three times and dried in an oven for 24 h at 100 °C.

The material after ion exchange was named Zn-X.

2.2 Drugs Sorption

Zoledronate sorption was initiated by introducing 20 mg of zinc zeolite into falcon polypropylene tubes. Each tube was filled with 15 ml of zoledronate solution with a concentration of 0.2 mg ml^{-1}. The samples were shaken for one week at room temperature then the samples were centrifuged. The amount of drug adsorbed on the carrier was determined by the difference between the amount of drug in the starting solution and the amount of drug remaining after sorption.

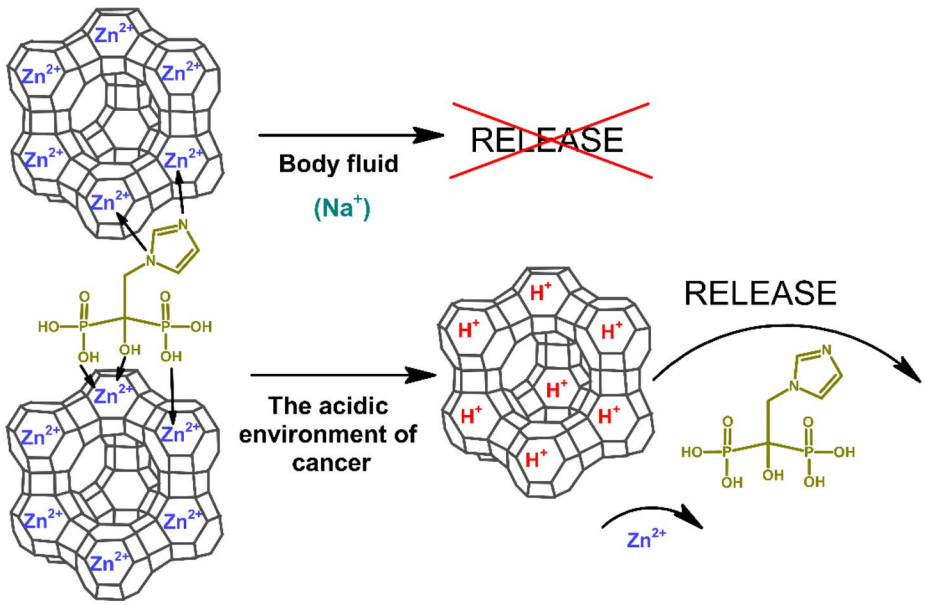

Fig. 1 The scheme of the research presented in this work

Six repetitions of drug sorption were performed to determine the reproducibility of this process.

The material after drug sorption was named Zn-X-ZOL.

The same procedure was used for Na-X zeolite, but the drug was not retained, and results for it are not presented.

2.3 Drug Release

Carrier after drug sorption was placed in 5 ml of simulated body fluid (SBF) or 5 ml of acetate buffer at 36.6 °C [18, 19]. The amount of drug released was measured using UV-VIS spectroscopy. Each time, the samples were centrifuged (5 min with 4500 rpm) and the fluid was replaced. Six repetitions of drug release were performed to determine the reproducibility of this process.

In the case of SBF, the samples were placed in solution for 100 h and the amount of drug released was measured every hour, then every 8 h, and then every 24 h. Due to the fact that the drug was not released during the entire process, the results were not presented.

In the case of the acetate buffer, the samples were placed in the solution for 15 min, after which the amount of released drug was tested. A new solution was then added and the amount of drug released was checked again after 15 min. The carrier was flooded a total of 9 times because no more drug was released after this time. The total release time was 135 min.

2.4 X-ray Diffractometry (XRD)

Samples were examined by X-ray diffraction using a D8 Advance diffractometer (Bruker) with a Johanson monochromator and a LynxEye detector. The measurement step was between 0.002 and 0.03, while the time for each step was between 2 and 3 s. Poly(methyl methacrylate) cuvettes were used during the tests. λCu Kα1 = 1.54 Å.

2.5 Scanning Electron Microscopy (SEM) and Energy Dispersive Spectroscopy (EDS)

SEM images were recorded with the use of scanning electron microscope VEGA 3 (TESCAN, Czech Republik). The SEM toll was equipped with an EDS analyzer (Bruker, UK). EDS was used to conduct the elemental analysis of the samples. The final concentration of each element was obtained by taking the average of measurements at 4 different spots.

2.6 Nitrogen Adsorption/Desorption Measurements

The nitrogen adsorption isotherm technique determined the BET surface area and pore parameters of obtained zeolites using an ASAP 2420 analyzer (Micromeritrics). Before experiments, the samples were outgassed at 200 °C in a vacuum chamber.

2.7 Fourier-Transform Infrared Spectroscopy

FT-IR analysis of all materials was performed using a Vertex70 spectrometer, Bruker Optics. All materials were studied using a single reflection diamond ATR crystal. The tests were carried out in the spectral range of $4000 - 600\ cm^{-1}$ with a resolution of $4\ cm^{-1}$ and 32 scans for signal accumulation.

2.8 Elemental Analysis

Measurements were performed on the FLASH 2000 elemental analyzer. Zeolite before and after sorption were weighed in tin capsules (approximately 2 mg) and introduced into the reactor by means of an autosampler together with an appropriate, precisely defined portion of oxygen. After combustion at a temperature of 900–1000 °C, the flue gases were transported in helium flow to the second furnace of the reactor filled with copper, and then through a water trap to the chromatographic column, which separates the individual products from each other. The separated gases were detected by a thermal conductivity detector.

2.9 UV-VIS Spectroscopy

UV-VIS spectrophotometer UV-2600 (Shimadzu, Japan) was applied for the determination of zoledronate concentration during sorption and release process. Measurements were made in the range of 212–240 nm (λ max = 217 nm) [20, 21].

2.10 Inductively Coupled Plasma mass Spectrometry (ICP-MS)

Measurements were carried out on a mass spectrometer with induction induced plasma ICP-MS NexION 300d by PerkinElmer. Liquid samples were subjected to quantitative analysis. For this purpose, a calibration curve was made and a zinc concentration was determined based on it. The analysis was performed in the KED system to avoid the matrix affecting the zinc content. The results were obtained in ppm.

3 Results

The first step in this work was to determine the effect of ion exchange on the faujasite structure. This was tested using XRD and the results are presented in Fig. 2. The shape of the Zn-X does not differ from Na-X zeolite. These results confirm that there is no influence of ion exchange with Zn^{2+}

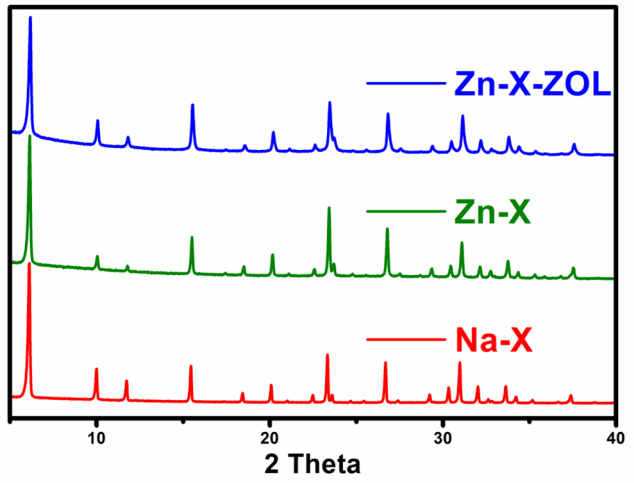

Fig. 2 X-ray diffraction patterns of Na-X, Zn-X, and Zn-X-ZOL zeolites

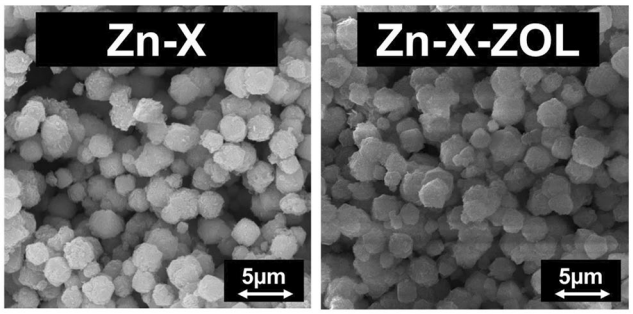

Fig. 3 SEM images for zinc zeolite before and after sorption of zoledronate

on the crystal structure of zeolite X. The lack of changes is important because in this work we want to prove that the incorporation of the zinc ion, and not the change of the zeolite structure, affects the sorption and release of the drug. In addition, it was checked whether the sorption of the drug affects the change in the crystalline properties of the material. As can be seen from Fig. 2, the results for Zn-X-ZOL are the same as for the other materials. This indirectly indicates that the drug did not crystallize, but was adsorbed through interactions with zinc ions.

Na-X zeolite particles used in this work have an average size of 2 μm. As can be seen in all SEM images, this value occurs also for Zn-X, both before and after zoledronate sorption (Fig. 3). The particles are very similar in size and appearance. This confirms that the incorporation of zinc ions and zoledronate does not affect the particle size and shape of zeolite [22]. The carrier after sorption of the zoledronate do not agglomerate. It indicates that the drug is probably present on the surface and in the pores of the zinc zeolite, rather than precipitated.

Table 1 Content of elements by weight based on EDS analysis [%]

	Na-X	Zn-X	Zn-X-ZOL
P	0	0	4.03 ± 2.11
N	0	0	2.90 ± 1.10
Zn	0	10.07 ± 4.47	11.04 ± 1.49
Na	11.32 ± 1.49	2.59 ± 0.93	2.44 ± 0.41

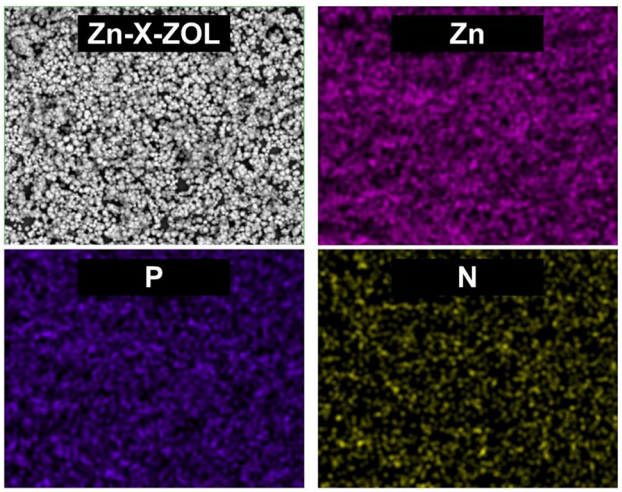

Fig. 4 SEM image of carrier after drug sorption and elemental mapping of the same region indicating the spatial distribution of zinc, phosphorus and nitrogen

The efficiency of ion exchange in sodium zeolite was confirmed by EDS analysis (Table 1). Comparison of ion content with the Na-X zeolite (Na ~ 11.3% wt %) shows that the ions only exchanged and did not e.g. precipitated out in a different form [23]. After ion exchange, no chloride is present in the zinc zeolite. EDS analysis, in addition to the effectiveness of ion exchange, also confirms the effectiveness of drug sorption. Effectiveness of sorption is demonstrated by the increase in the amount of phosphorus and nitrogen. Both these elements are not present in the surface layer before sorption of the drug and significant amounts can be observed after that process.

The distribution of the drug on the carrier surface was performed using EDS mapping (Fig. 4). As can be seen from the distribution of all elements, zoledronate is visible on the entire surface of the carrier. Drug adsorption is proved by the presence of phosphorous and nitrogen, which are present in the structure of zoledronate.

The Nitrogen Adsorption / Desorption results are shown in Table 2. After ion exchange with zinc ions, a decrease in the value of the specific surface area and the pore volume can be seen. This is a typical phenomenon and has already been described in the literature [24, 25]. The specific surface area of carrier drops significantly after drug sorption (about 24%). The decrease is due to the surface being covered with the ZOL layer. As can be seen, the number of micropores

Table 2 Characteristics of Materials Based on Nitrogen Adsorption / Desorption Measurements

	Na-X	Zn-X	Zn-X-ZOL
BET surface area [$m^2 \cdot g^{-1}$]	645.33	568.46	434.25
t-Plot Micropore Area [$m^2 \cdot g^{-1}$]	607.46	501.65	294.27
Total pore volume [$cm^3 \cdot g^{-1}$]	0.326	0.312	0.281
t-Plot micropore volume [$cm^3 \cdot g^{-1}$]	0.298	0.246	0.144

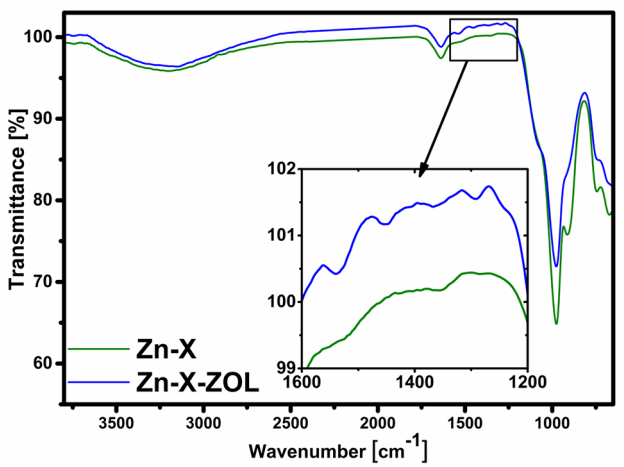

Fig. 5 IR spectra for zinc zeolite before and after sorption of zoledronate

Table 3 Elemental analysis of carrier before and after drug sorption

	C	N
Zn-X	0.10 ± 0.01	0
Zn-X-ZOL	2.80 ± 0.13	0.64 ± 0.10

is several times greater for Zn-X material than the number of other pores. After drug sorption, the following decrease in micropore area was observed for zeolite Zn-X (207.38 $m^2 \cdot g^{-1}$). Large changes are also noticeable in the volume of micropores. For zeolite Zn-X, the volume of micropores decreased by 0.102 $cm^3 \cdot g^{-1}$. The obtained results confirm the effectiveness of zoledronate sorption on zinc zeolite.

Another technique used in the characterization of the materials was IR spectroscopy (Fig. 5). The spectrum after ion exchange is typical of FAU zeolite. The first two bands at 3400 cm^{-1} and 1640 cm^{-1} are assigned to the absorbed water and hydroxyl groups on the surface of the zeolite. The main confirmation of the FAU structure are the bands in the range of 1200 – 600 cm^{-1}. The strong and broad band in the range 1200 – 900 cm^{-1} is assigned to the asymmetric internal T-O stretching vibrations of the TO_4 tetrahedra. The two bands between 800 and 650 cm^{-1} are assigned to the stretching vibration of Al-O in the Si-O-Al bonds [26, 27]. New bands characteristic for organic compounds are visible after sorption of the zoledronate. Bands in the range 1580–1320 cm^{-1} can be assigned to C = C and C = N stretch vibrations [28, 29]. These bands are derived from the

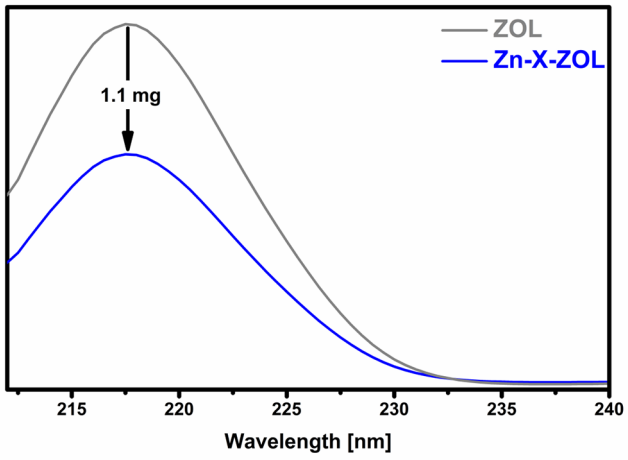

Fig. 6 Sorption of zoledronate ("ZOL" means starting solution)

imidazolium ring. The bands found at 1290 cm^{-1} possibly arise due to P = O stretching vibrations [30, 31].

The results of the elemental analysis also confirm the effectiveness of drug sorption in the prepared materials (Table 3). This is evidenced by the increase in the amount of carbon and nitrogen compared to zeolites prior to sorption.

The exact amount of drug retained on the carrier was determined using UV-Vis analysis (Fig. 6). Approximately 1.1 mg of the drug was retained in 20 mg of carrier. The amount of drug retained on the carrier was determined based on the amount of drug remaining in the starting solution. The 5% drug content on the carrier surface can be considered high content. But of course it is more important whether such a carrier-drug system is stable and the drug is not released into healthy human tissues. This feature can only be proven when released in an appropriate environment: in SBF or in the cancer environment.

The amount of drug retained on the carrier surface is very important. However, more important is whether the drug is released, because only then can it act on diseased cells. Only one release profile can be seen in the presented chart (Fig. 7). This is because the drug is not released under the influence of SBF. This proves the assumption presented in this paper. We have prepared a material that will not release the drug under the influence of body fluids, and thus will not affect healthy organs. We studied drug release under SBF for over 100 h and no drug release was observed. This proves high stability and the fact that our system is not toxic and affects only cancer cells in the human body. Such material can be safely removed from the body without adversely affecting other organs. This is because zeolite X (FAU) is considered biocompatible. Lutzweiler et al. proved that magnesium and calcium zeolites do not have cytotoxic properties [32]. Cytotoxicity studies were also carried out for the zinc zeolite described in this paper. The absence of zeolite toxicity was proven using MCF-7 cells [33].

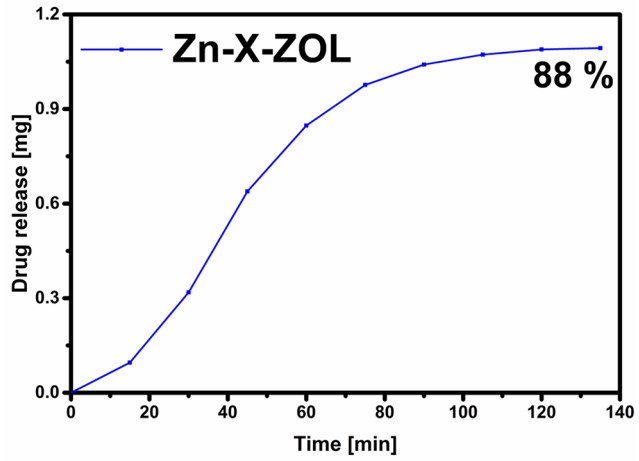

Fig. 7 Total release of zoledronate from the zinc zeolite under the influence of acetate buffer

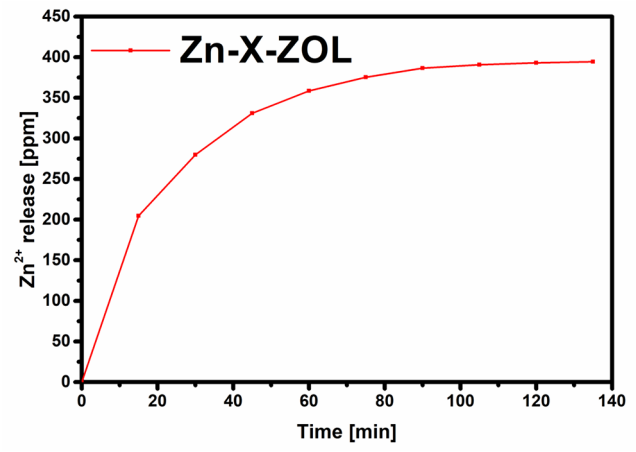

Fig. 8 Total release of zinc ions (Zn^{2+}) from the zinc zeolite with drug under the influence of acetate buffer

Importantly, our material releases the drug in contact with the cancer environment in about 2 h. Looking at the profile, it is obvious that the material proposed in this paper targets the cancer environment. As can be seen in the first 15 min, the dose is lower. This is only because the acidic environment must reach the active sites in the zeolite structure. Importantly, during about 2 h, the carrier released almost 88% of the drug.

Zoledronate is released only in cancer environment from zinc zeolites because zoledronate have a nitrogen atom in structure with a free electron pair, which can potentially bind with zinc ions, which slows down the release [34–36].

Comparing our material to those known by us and presented in the literature, it can be concluded that the material presented in this work has a greater application potential. For example, Cai et all. presented the material - hydroxyapatite loaded polymeric nanoparticles and investigated the effect of pH on zoledronate release [37]. These studies determined that release was influenced by pH, but drug was released at both pH 7.4 and pH 5.0. Which proves that the drug will reach both healthy and affected cells. Another example is calcium zoledronate nanoscale Metal-Organic Frameworks prepared by Au et all. [5]. This interesting study confirmed that the creation of MOFs allows more drug to be released in an acidic environment. However, the release lasted for 24 h which is a long time for the target drug release. In addition, 5% of the drug was also released at pH 7.4 within 24 h, so this material was not totally nontoxic to healthy tissues. Xiao et all. obtained hybrid polymeric nanoparticles with high zoledronic acid loading [38]. The production of this material made it possible to increase the release in an acidic environment. However, as in the previous examples, the drug was also released at pH = 7.4. Benyettou et all. prepared a magnetic nanoparticle-based drug delivery system [39]. The material they produced did not release the drug at pH = 7.4. The drug was released at pH = 5.4. However, the drug was released uncontrolled. 36.6% of the drug being released immediately and 73.5% being released gradually within four days. From the presented examples it can be seen that the materials designed so far did not contain both important features in targeted release. The material presented in this work has both features: no release of drug at pH = 7.4, and very fast drug release in an acidic environment.

During the research, the amount of zinc released from the carrier was also determined (Fig. 8). As in the case of the drug, zinc ions are quickly released under the influence of an acidic environment. This is desirable because the large amount of ions released in the environment of the cancer can affect the induction of cancer apoptosis cells by increasing the intracellular production of reactive oxygen species [17]. The release of drug and ions at the disease site indicates a double therapeutic effect of the prepared material.

4 Conclusion

Zinc form of zeolite X was used as carrier for the zoledronate. The results presented in this study confirm the effectiveness of ion exchange and drug sorption. The morphological properties of the material after sorption did not change, which proves that the drug is attached to zinc ions in the zeolite structure, and not precipitated. The sorption efficiency was confirmed by the presence of nitrogen and phosphorus ions in the analyzed samples. The carrier is capable of retaining about 5% of the drug, based on the weight of the carrier. Most importantly, the drug is released only in an acidic environment (cancerous environment). At a pH of 7.4, the drug is not released at all, which confirms that it will not affect healthy human cells. A comparison of

our material with literature reports shows its great potential. To our knowledge, no material has yet been developed that would release the drug in a very short time and only in an acidic environment. Moreover, this material releases zinc ions which additionally act on cancer cells by induction apoptosis of cancer cells by increasing the intracellular production of reactive oxygen species [17]. This is the first report on this type of material. In the next stages of research in the future, we will focus on the preparation of zoledronate retained zinc nanozeolites and determine their effect on cancer cells in in vivo studies.

Acknowledgements Mariusz Sandomierski was supported by the Foundation for Polish Sciences (FNP).

Author Contribution M.S. Conceptualization, Methodology, Validation, Investigation, Writing - Original Draft; M.J. Methodology, Investigation; M.R. Investigation; M.P. Investigation; A.V. Resources, Supervision.

Funding This research was funded by the Ministry of Education and Science (Poland).

Declarations

Conflict of Interest There are no conflicts of interest to declare.

References

1. N.B. Watts, D.L. Diab, Long-term use of bisphosphonates in osteoporosis. J. Clin. Endocrinol. Metab. **95**, 1555–1565 (2010). https://doi.org/10.1210/jc.2009-1947
2. M.J. Rogers, S. Gordon, H.L. Benford, F.P. Coxon, S.P. Luckman, J. Monkkonen, J.C. Frith, Cellular and molecular mechanisms of action of bisphosphonates, Cancer. 88 (2000) 2961–2978. https://doi.org/10.1002/1097-0142(20000615)88:12+<2961::aid-cncr12>3.3.co;2-c
3. R.G.G. Russell, Bisphosphonates: the first 40 years. Bone. **49**, 2–19 (2011). https://doi.org/10.1016/j.bone.2011.04.022
4. J. Green, A. Lipton, Anticancer properties of zoledronic acid. Cancer Invest. **28**, 944–957 (2010). https://doi.org/10.3109/07357907.2010.512598
5. N.M. La-Beck, X. Liu, H. Shmeeda, C. Shudde, A.A. Gabizon, Repurposing amino-bisphosphonates by liposome formulation for a new role in cancer treatment. Semin. Cancer Biol. **68**, 175–185 (2021). https://doi.org/10.1016/j.semcancer.2019.12.001
6. K.M. Au, A. Satterlee, Y. Min, X. Tian, Y.S. Kim, J.M. Caster, L. Zhang, T. Zhang, L. Huang, A.Z. Wang, Folate-targeted pH-responsive calcium zoledronate nanoscale metal-organic frameworks: turning a bone antiresorptive agent into an anticancer therapeutic. Biomaterials. **82**, 178–193 (2016). https://doi.org/10.1016/j.biomaterials.2015.12.018
7. A.P. Soares, R.F. do Espírito, S.R.P. Santo, M. Line, G.F. das, PdeM. Pinto, M.B.P. Santos, A.R. Toralles, Do Espírito Santo, Bisphosphonates: Pharmacokinetics, bioavailability, mechanisms of action, clinical applications in children, and effects on tooth development. Environ. Toxicol. Pharmacol. **42**, 212–217 (2016). https://doi.org/10.1016/j.etap.2016.01.015
8. R.E. Coleman, E.V. McCloskey, Bisphosphonates in oncology. Bone. **49**, 71–76 (2011). https://doi.org/10.1016/j.bone.2011.02.003
9. M. Pazianas, B. Abrahamsen, Safety of bisphosphonates. Bone. **49**, 103–110 (2011). https://doi.org/10.1016/j.bone.2011.01.003
10. E. Boedtkjer, S.F. Pedersen, The acidic Tumor Microenvironment as a driver of Cancer. Annu. Rev. Physiol. **82**, 103–126 (2020). https://doi.org/10.1146/annurev-physiol-021119-034627
11. B. Lin, H. Chen, D. Liang, W. Lin, X. Qi, H. Liu, X. Deng, Acidic pH and High-H2O2 dual Tumor Microenvironment-Responsive Nanocatalytic Graphene Oxide for Cancer Selective Therapy and Recognition. ACS Appl. Mater. Interfaces **11**, 11157–11166 (2019). https://doi.org/10.1021/acsami.8b22487
12. L. Bacakova, M. Vandrovcova, I. Kopova, I. Jirka, Applications of zeolites in biotechnology and medicine – a review. Biomater. Sci. **6**, 974–989 (2018). https://doi.org/10.1039/C8BM00028J
13. H. Serati-Nouri, A. Jafari, L. Roshangar, M. Dadashpour, Y. Pilehvar-Soltanahmadi, N. Zarghami, Biomedical applications of zeolite-based materials: a review. Mater. Sci. Eng. C **116**, 111225 (2020). https://doi.org/10.1016/j.msec.2020.111225
14. M. Król, Natural vs. Synthetic Zeolites, Crystals. 10 (2020) 622. https://doi.org/10.3390/cryst10070622
15. X. Xu, J. Wang, Y. Long, Zeolite-based materials for gas sensors. Sensors. **6**, 1751–1764 (2006). https://doi.org/10.3390/s6121751
16. M. Sandomierski, M. Zielińska, A. Voelkel, Calcium zeolites as intelligent carriers in controlled release of bisphosphonates. Int. J. Pharm. **578**, 119117 (2020). https://doi.org/10.1016/j.ijpharm.2020.119117
17. M. Provinciali, A. Donnini, K. Argentati, G. Di Stasio, B. Bartozzi, G. Bernardini, Reactive oxygen species modulate Zn2+-induced apoptosis in cancer cells. Free Radic. Biol. Med. **32**, 431–445 (2002). https://doi.org/10.1016/S0891-5849(01)00830-9
18. R.K. Thapa, Y. Choi, J.-H. Jeong, Y.S. Youn, H.-G. Choi, C.S. Yong, J.O. Kim, Folate-Mediated Targeted Delivery of Combination Chemotherapeutics Loaded Reduced Graphene Oxide for Synergistic Chemo-Photothermal Therapy of Cancers, Pharm. Res. 33 (2016) 2815–2827. https://doi.org/10.1007/s11095-016-2007-0
19. M. Pietrzyńska, A. Voelkel, Stability of simulated body fluids such as blood plasma, artificial urine and artificial saliva. Microchem J. **134**, 197–201 (2017). https://doi.org/10.1016/j.microc.2017.06.004
20. D.K. Khajuria, R. Razdan, Sensitive and R.P.-H.P.L.C. Rapid Quantification of Zoledronic Acid in a hydroxyapatite-based nanoparticles, Indian J. Pharm. Sci. 79 (2017). https://doi.org/10.4172/pharmaceutical-sciences.1000262
21. D. Liu, S.A. Kramer, R.C. Huxford-Phillips, S. Wang, J.D. Rocca, W. Lin, Coercing bisphosphonates to kill cancer cells with nanoscale coordination polymers. Chem. Commun. **48**, 2668–2670 (2012). https://doi.org/10.1039/C2CC17635A
22. B. Kwakye-Awuah, C. Williams, M.a. Kenward, I. Radecka, Antimicrobial action and efficiency of silver-loaded

zeolite X. J. Appl. Microbiol. **104**, 1516–1524 (2008). https://doi.org/10.1111/j.1365-2672.2007.03673.x
23. Z. Buchwald, M. Sandomierski, A. Voelkel, Calcium-Rich 13X Zeolite as a filler with remineralizing potential for Dental Composites, ACS Biomater. Sci. Eng. **6**, 3843–3854 (2020). https://doi.org/10.1021/acsbiomaterials.0c00450
24. J. Liu, N. He, Z. Zhang, J. Yang, X. Jiang, Z. Zhang, J. Su, M. Shu, R. Si, G. Xiong, H. Xie, G. Vilé, Highly-dispersed zinc species on Zeolites for the continuous and selective dehydrogenation of ethane with CO_2 as a Soft oxidant. ACS Catal. **11**, 2819–2830 (2021). https://doi.org/10.1021/acscatal.1c00126
25. S. Chen, J. Popovich, W. Zhang, C. Ganser, S.E. Haydel, D.-K. Seo, Superior ion release properties and antibacterial efficacy of nanostructured zeolites ion-exchanged with zinc, copper, and iron, RSC Adv. 8 (n.d.) 37949–37957. https://doi.org/10.1039/c8ra06556j
26. J. Xie, W. Meng, D. Wu, Z. Zhang, H. Kong, Removal of organic pollutants by surfactant modified zeolite: comparison between ionizable phenolic compounds and non-ionizable organic compounds, J. Hazard. Mater. 231–232 (2012) 57–63. https://doi.org/10.1016/j.jhazmat.2012.06.035
27. D. Wu, Y. Lu, H. Kong, C. Ye, X. Jin, Synthesis of Zeolite from thermally treated sediment. Ind. Eng. Chem. Res. **47**, 295–302 (2008). https://doi.org/10.1021/ie071063u
28. S. Chen, P. Wan, B. Zhang, K. Yang, Y. Li, Facile fabrication of the zoledronate-incorporated coating on magnesium alloy for orthopaedic implants. J. Orthop. Transl **22**, 2–6 (2020). https://doi.org/10.1016/j.jot.2019.09.007
29. D.K. Khajuria, R. Razdan, D.R. Mahapatra, Development, in vitro and in vivo characterization of zoledronic acid functionalized hydroxyapatite nanoparticle based formulation for treatment of osteoporosis in animal model. Eur. J. Pharm. Sci. Off J. Eur. Fed. Pharm. Sci. **66**, 173–183 (2015). https://doi.org/10.1016/j.ejps.2014.10.015
30. M.M. Prasanthi, B.A. Rao, B.V.N. Rao, Y.P. Krishna, D.V. Ramana, FORMULATION AND EVALUATION OF ZOLEDRONIC ACID FOR INJECTION BY LYOPHILIZATION TECHNIQUE, Int. Res. J. Pharm. **8**, 50–56 (2017). https://doi.org/10.7897/2230-8407.080224
31. G. Boran, S. Tavakoli, I. Dierking, A. Kamali, D. Ege, Synergistic effect of graphene oxide and zoledronic acid for osteoporosis and cancer treatment, Sci. Rep. 10 (2020). https://doi.org/10.1038/s41598-020-64760-4
32. G. Lutzweiler, Y. Zhang, F. Gens, A. Echalard, G. Ladam, J. Hochart, T. Janicot, N. Mofaddel, B. Louis, Deciphering the role of faujasite-type zeolites as a cation delivery platform to sustain the functions of MC3T3-E1 pre-osteoblastic cells, mater. Adv. (2022). https://doi.org/10.1039/D2MA00768A
33. M. Jakubowski, M. Kucinska, M. Ratajczak, M. Pokora, M. Murias, A. Voelkel, M. Sandomierski, Zinc forms of faujasite zeolites as a drug delivery system for 6-mercaptopurine. Microporous Mesoporous Mater. **343**, 112194 (2022). https://doi.org/10.1016/j.micromeso.2022.112194
34. E. Freire, D.R. Vega, R. Baggio, Zoledronate complexes. III. Two zoledronate complexes with alkaline earth metals: [Mg(C5H9N2O7P2)2(H2O)2] and [Ca(C5H8N2O7P2)(H2O)]n, Acta Crystallogr. Sect. C **66**, m166–m170 (2010). https://doi.org/10.1107/S0108270110017634
35. E. Freire, D.R. Vega, Aquabis[1-hydroxy-2-(imidazol-3-ium-1-yl)-1,1'-ethylidenediphophonato-κO,o']zinc(II) dihydrate, Acta Crystallogr. Sect. E Struct. Rep. Online **65**, m1430–1431 (2009). https://doi.org/10.1107/S160053680904286X
36. M. Vassaki, K.E. Papathanasiou, C. Hadjicharalambous, D. Chandrinou, P. Turhanen, D. Choquesillo-Lazarte, K.D. Demadis, Self-sacrificial MOFs for ultra-long controlled release of bisphosphonate anti-osteoporotic drugs. Chem. Commun. **56**, 5166–5169 (2020). https://doi.org/10.1039/D0CC00439A
37. Y. Cai, T. Gao, S. Fu, P. Sun, Development of zoledronic acid functionalized hydroxyapatite loaded polymeric nanoparticles for the treatment of osteoporosis. Exp. Ther. Med. **16**, 704–710 (2018). https://doi.org/10.3892/etm.2018.6263
38. M.-C. Xiao, Y.-H. Chou, Y.-N. Hung, S.-H. Hu, W.-H. Chiang, Hybrid polymeric nanoparticles with high zoledronic acid payload and proton sponge-triggered rapid drug release for anticancer applications. Mater. Sci. Eng. C **116**, 111277 (2020). https://doi.org/10.1016/j.msec.2020.111277
39. F. Benyettou, M. Alhashimi, M. O'Connor, R. Pasricha, J. Brandel, H. Traboulsi, J. Mazher, J.-C. Olsen, A. Trabolsi, Sequential delivery of Doxorubicin and Zoledronic acid to breast Cancer cells by CB[7]-Modified Iron oxide nanoparticles. ACS Appl. Mater. Interfaces **9**, 40006–40016 (2017). https://doi.org/10.1021/acsami.7b11423